Interconversion of the Ligand Arrays in the CD and EF Sites of Oncomodulin. Influence on Ca^{2+}-Binding Affinity†

Michael T. Henzl,*,‡ Raymond C. Hapak,‡ and John J. Likos§

Department of Biochemistry, University of Missouri−Columbia, Columbia, Missouri 65211, and Monsanto Corporate Research, St. Louis, Missouri 63198

Received December 23, 1997; Revised Manuscript Received April 20, 1998

ABSTRACT: The parvalbumin metal ion-binding sites differ at the $+z$ and $-x$ residues: Whereas the CD site employs serine and glutamate (or aspartate), respectively, the EF site employs aspartate and glycine. Although frequently indistinguishable in Ca^{2+}- and Mg^{2+}-binding assays, the CD and EF sites nonetheless exhibit markedly different preferences for members of the lanthanide series [Williams et al. (1984) *J. Am. Chem. Soc. 106*, 5698−5702], underscoring an intrinsic nonequivalence. This nonequivalence reaches its pinnacle in the mammalian β-parvalbumin (oncomodulin). Whereas the oncomodulin EF site exhibits the expected Ca^{2+}/Mg^{2+} signature, the Ca^{2+} affinity of the CD site is severely attenuated. To obtain insight into the structural factors responsible for this reduction in binding affinity, oncomodulin variants were examined in which the CD and EF site ligand arrays had been exchanged. Our data suggest that binding affinity may be dictated either by ligand identity or by the binding site environment. For example, the Ca^{2+} affinity of the quasi-EF site resulting from the combined S55D and D59G mutations is substantially lower than that of the authentic EF site. This finding implies that other local environmental variables (e.g., binding loop flexibility, electrostatic potentials) within the CD binding site supersede the influence of ligand identity. However, the CD site ligand array does not acquire a high-affinity signature when imported into the EF site, as in the D94S/G98D variant. Instead, it retains its Ca^{2+}-specific signature, implying that this constellation of ligands is less sensitive to placement within the protein molecule. The D59G and D94S single mutations substantially lower binding affinity, consistent with removal of a liganding carboxylate. By contrast, the S55D and G98D mutations substantially increase binding affinity, a finding at odds with corresponding data collected on model peptide systems. Significantly, the Ca^{2+} affinity of the oncomodulin CD site is increased by mutations that weaken binding at the EF site, indicating a negatively cooperative interaction between the two sites.

The "EF-hand" metal ion-binding motif consists of a 12-residue binding loop flanked by short helical segments (*1*, *2*). The coordinating ligands are invariably oxygen atoms—carboxylate, hydroxyl, carbonyl, or aquo—and are arrayed at the vertexes of a pentagonal bipyramid. Despite their general similarity, individual EF-hand domains exhibit substantial variation in their ion-binding properties. Clearly, the fundamental determinants of metal ion-binding affinity in these proteins must be identical to those that govern binding to small organic chelators, i.e., ion size and charge. However, it is apparent that affinity can be modulated by diverse mechanisms in protein systems, so that a quantitative understanding of the relationship between protein structure and Ca^{2+}-binding behavior remains well out of reach (*3*, *4*). The small (M_r 12 000) vertebrate-specific proteins called parvalbumins (*5*−*8*) offer an attractive system for exploring this issue.

Parvalbumins contain two functional Ca^{2+}-binding sites called the CD[1] and EF sites, a reference to the helices flanking the central binding loops. The CD-binding loop is positioned in the center of the protein sequence, spanning residues 51−62; the EF loop is positioned near the C-terminus, spanning residues 90−101. Although the two sites are typically indistinguishable in Ca^{2+}-binding assays (9−12), they differ significantly in their interactions with the lanthanide series. Whereas the EF site is flexible, accommodating the various members of the series with comparable affinities, the CD site evinces a strong preference for the larger ions at the beginning of the series (*13*).

The parvalbumin (PV) family includes α and β sublineages (*14*, *15*). The α isoforms are less acidic (pI > 5.0) and have an additional residue in the C-terminal helix. Regardless of source, they exhibit very high affinity for Ca^{2+} ($K_{Ca} < 10^{-8}$ M) and physiologically significant affinity for Mg^{2+} ($K_{Mg} < 10^{-4}$ M). These metal ion-binding properties are consistent with a Ca^{2+} buffering function. The mammalian α-PV

† This work was supported by NSF Awards MCB9296171 and MCB9603877 (to M.T.H.). Portions of this work were presented at the Tenth International Symposium on Calcium-Binding Proteins in Health and Disease, Lund, Sweden, June 17−21, 1997.

* To whom correspondence should be addressed. Telephone: 573-882-7485. Fax: 573-884-4812. E-mail: bchenzl@muccmail.missouri.edu.

‡ University of Missouri−Columbia.

§ Monsanto Corporate Research.

[1] Abbreviations: CD site, the parvalbumin metal ion-binding site flanked by the C and D helical segments; EF site, metal ion-binding site flanked by the E and F helical segments; EDTA, ethylenediaminetetraacetic acid; Hepes, 4-(2-hydroxyethyl)-1-piperazineethanesulfonic acid; PV, parvalbumin; OM, oncomodulin; wt, wild-type.

S0006-2960(97)03151-6 CCC: $15.00
Published on Web 06/05/1998

is expressed in diverse tissue settings (*16*). It is particularly abundant (>1 mM) in fast-twitch skeletal muscle (*17*), where it is believed to facilitate relaxation. Consistent with this hypothesis, Müntener et al. (*18*) have recently shown that the myofibrillar relaxation rate is accelerated by direct injection of parvalbumin cDNA. The protein is also expressed at moderate levels—approximately 50 μM (*19*)—in rapidly firing neurons, particularly GABA-ergic neurons (*20*, *21*). In the latter setting, PV may confer protection against Ca^{2+} toxicity (*22*).

In contrast to the α isoform, postnatal expression of the mammalian β-PV is apparently confined to the outer hair cells of the mammalian auditory organ, the Organ of Corti (*23*−*25*). In rat, the protein has also been detected in the pre-implantation embryo and placenta (*26*, *27*). Due to its frequent expression in neoplasms (*8*, *28*, *29*), the mammalian β-PV is commonly called oncomodulin (OM). The physiological role of OM is presently conjectural. It may function as a tissue-specific Ca^{2+}-dependent regulatory protein. Blum and Berchtold (*30*) have shown, for example, that the cell-cycle length of a tumor cell line is sensitive to the expression level of the protein. Alternatively, OM may serve as a specialized cytosolic Ca^{2+} buffer.

Relative to the α-PVs, the β lineage exhibits greater diversity in metal ion-binding behavior. OM, for example, displays substantially reduced affinity for Ca^{2+} (*31*, *32*). In fact, with an apparent dissociation constant for Ca^{2+} of 0.8 μM, the CD site qualifies as a "Ca^{2+}-specific site." Moreover, the relative rigidity of the CD site is exaggerated in OM (*33*). In previous studies undertaken by this laboratory to identify the underlying structural basis for this behavior, the OM codon was replaced with the corresponding rat muscle parvalbumin (RPV) codon at selected positions of nonidentity. Ca^{2+}-binding data for the resulting proteins suggested that the attenuation of ion-binding affinity results from multiple substitutions both within and outside the binding pockets (*34*, *35*).

Cox, Berchtold, and co-workers have also studied the metal ion-binding properties of OM and RPV. In one study (*36*), they examined alterations in metal ion-binding affinity resulting from simultaneous RPV→OM mutations at four hydrophobic residues in the CD domain of RPV (V46I, L50I, I58L, and I66F). Their data suggested that the combined mutations afford increased selectivity toward Ca^{2+}. In a companion study (*37*), they produced chimeras of RPV and OM—[S41-Q71]RPV and [D41-S71]OM, respectively—in which the entire CD domain (residues 41−71) was replaced with the corresponding domain from the other protein. Binding data indicated that the CD site of [S41-Q71]RPV had acquired metal ion-binding properties resembling those of OM. Similarly, the CD site of [D41-S71]OM appeared to have acquired properties resembling those of RPV. The investigators concluded that the Ca^{2+}-specificity of the oncomodulin CD site is an intrinsic property of the site, i.e., that the specificity is largely dictated by the local sequence.

To further delineate the relative importance of structural determinants beyond the immediate coordination sphere, we have inserted the EF ligand array of OM into the CD-binding loop. The resulting protein contains, in effect, two EF sites, and their relative Ca^{2+} affinities can potentially furnish insight into the structural preference of this ligand array. At one extreme, if the binding properties of this particular Ca^{2+}-binding domain were dictated exclusively by the coordinating residues, the wild-type and engineered sites should exhibit the same affinity. At the other, if higher order structural considerations figure prominently, then substantially different binding properties may be observed.

We have likewise examined the consequences of inserting the CD ligand array into the EF-binding loop—in effect creating a protein with two CD sites—as well as the consequences of exchanging the CD and EF ligand arrays. Finally, we have characterized the Ca^{2+}-binding properties for each of the individual mutations. The influence of these site-specific modifications on Eu^{3+} luminescence behavior has been described elsewhere (*38*).

MATERIALS AND METHODS

Recombinant OM was expressed in *Escherichia coli* DH5α harboring the pLD2 expression vector. pLD2 is a derivative of pBluescript (Stratagene Corp., La Jolla, CA), in which the OM coding sequence has been placed downstream from the *lac* promoter. Alterations in the OM coding sequence were introduced by oligonucleotide-directed mutagenesis, employing a double-stranded template (*39*). One-liter LB broth cultures yielded 50−100 mg of purified protein. The recombinant proteins were isolated as previously described (*31*).

Divalent cations were scavenged from protein preparations and buffers alike by passage over columns of EDTA-derivatized agarose (*40*). Typically, 0.5 mL of EDTA−agarose was employed per milligram of protein. For the S55D and G98D variants, however, this ratio was increased to 2.0 mL of resin per milligram of protein, due to their substantially higher Ca^{2+}-binding affinities. Treatment with this chelating matrix removed >98% of the bound Ca^{2+}, as judged by flame atomic absorption measurements. Protein concentrations were estimated by UV absorbance, employing an extinction coefficient of 3260 M^{-1} cm^{-1}.

Flow-dialysis measurements (*41*, *42*) were conducted on 100 μM protein samples in 0.15 M NaCl, 0.025 M Hepes−NaOH, pH 7.4, at 25 °C, as described previously (*31*, *34*). For those mutations that severely reduced one of the Ca^{2+}-binding constants, an abbreviated titration protocol was employed, to prevent depletion of the label. Dissociation constants were extracted by fitting the data to the sum of two hyperbolas:

$$r = \frac{[Ca^{2+}]}{k_1 + [Ca^{2+}]} + \frac{[Ca^{2+}]}{k_2 + [Ca^{2+}]}$$

In this equation, r is the average binding number, and k_1 and k_2 are the apparent dissociation constants for the two binding sites. Least-squares analyses were performed with Scientist (Micro-Math Inc., Salt Lake City, UT). The reported dissociation constants represent the mean of at least three determinations.

Titration Calorimetry. Ca^{2+} titrations were monitored calorimetrically at 25 °C in an isothermal titration calorimeter from Calorimetry Sciences Corp. (Provo, UT). Following equilibration, 4.0 μL additions of titrant were made automatically to the 1.00 mL sample at 200 s intervals from a 100 μL Hamilton syringe driven by a precision stepping motor. In all cases, the sample buffer consisted of 0.15 M NaCl,

0.025 M Hepes−NaOH, pH 7.4. The reference cell contained 1.00 mL of water.

Raw voltage data were integrated using ITC Dataworks (v. 1.0, Applied Thermodynamics). Prior to least-squares analysis, the data were corrected for the heats of mixing and titrant dilution by subtracting a blank titration, i.e., titration of buffer alone. Enthalpies of binding were extracted from the data using BindWorks (v. 1.0b, Applied Thermodynamics). The analyses utilized the following model describing two classes of independent binding sites (*43*):

$$Q = Q_1 + Q_2 = (\Delta H_1[L_{B,1}] + \Delta H_2[L_{B,2}])\cdot V \quad (1)$$

$$Q = V[M]\left(\frac{n_1\Delta H_1 K_1[L]}{1 + K_1[L]} + \frac{n_2\Delta H_2 K_2[L]}{1 + K_2[L]}\right) \quad (2)$$

$$[L_{B,1}] = [M]\left(\frac{n_1\Delta H_1 K_1[L]}{1 + K_1[L]}\right); [L_{B,2}] = [M]\left(\frac{n_2\Delta H_2 K_2[L]}{1 + K_2[L]}\right) \quad (3)$$

$$[L] = [L_T] - [M]\left(\frac{n_1 K_1[L](1 + K_2[L]) + n_2 K_2[L](1 + K_1[L])}{(1 + K_1[L])(1 + K_2[L])}\right) \quad (4)$$

The subscripts 1 and 2 denote the two classes of binding site. n_1 and n_2 are the number of sites in each class. ΔH and K represent the molar enthalpy of ligand binding and the ligand association constant, respectively. [L] is the free ligand concentration. $[L_{B,1}]$ and $[L_{B,2}]$ represent the concentrations of ligand bound at each of the two classes of site. [M] is the total protein concentration. V is the sample volume. Q, Q_1, and Q_2 represent the total heat of binding and the heats associated with the binding events at each class of site.

For the least-squares analyses, the binding constants were fixed at the values obtained by direct binding studies. R^2, as defined below, exceeded 0.99 in all cases.

$$R^2 = \frac{\left|\sum_{i=1}^{n} {Y_{obs_i}}^2 - \sum_{i=1}^{n}(Y_{obs_i} - Y_{cal_i})^2\right|}{\sum_{i=1}^{n} {Y_{obs_i}}^2} \quad (5)$$

Y_{obs} and Y_{cal} represent the observed and calculated values, respectively, for a particular data point.

The heat of protonation of tris(hydroxymethyl)aminomethane was used for calibration. At 25 °C, this quantity is −11.36 kcal/mol (*44*). The calorimeter performance was evaluated by titrating 18-crown-6 with Ba^{2+}. The enthalpy and dissociation constants for this reaction are -7.47 ± 0.095 kcal/mol and $(1.74 \pm 0.39) \times 10^{-4}$ M, respectively (*45*).

Scanning calorimetry was performed on the apo-proteins in a Nano-DSC (Calorimetry Sciences Corp. and Applied Thermodynamics). Prior to analysis, the samples were dialyzed to equilibrium against 0.20 M NaCl, 10 mM EDTA, pH 7.4. All of the data presented were collected at a scan rate of 60 °C per hour, after verifying that the line width of the thermal transition and excess heat capacity were independent of scan rate for the wild-type protein. Data analysis was performed with CpCalc (v.2.0, Applied Thermodynamics).

NMR spectroscopy was conducted, at 37 °C, on 2−4 mM samples of the variant proteins in 0.15 M NaCl, pH 6.0, containing 10% D_2O. Data were collected on a Varian UNITY-500 spectrometer and processed with TRIAD (Tripos, Inc., St. Louis, MO) or VNMR (Varian Instruments, Palo Alto, CA) software. ^1H shifts were referenced to the absolute ^1H frequency of 0.1% TSP in D_2O. Clean-TOCSY (*46*) datasets were acquired on the apo-protein and following addition of 0.5 and 2.0 molar equiv of Ca^{2+}. The order of occupancy was apparent from the magnitudes of select resonances in the CD- and EF-binding sites. The spectral width was 7000 Hz in both dimensions, with 1024 complex points in t_2 and 256 complex FIDs in t_1. The carrier frequency was centered on the water signal, which was suppressed by selective irradiation during the relaxation delay of 1 s. The mixing time was 60 ms.

RESULTS

The liganding residues within an EF-hand domain—roughly positioned at the vertexes of an octahedron—are denoted (from N- to C-terminal) as $+x$, $+y$, $+z$, $-y$, $-x$, and $-z$ (e.g., *1*). In the oncomodulin CD site, the $+x$, $+y$, $+z$, and $-z$ ligands are donated by the side chains of Asp, Asp, Ser, and Glu, respectively (Figure 1). The $-y$ ligand, as in all canonical EF-hands, is a peptide backbone carbonyl, in this case the carbonyl of Tyr-57. The $-x$ residue is an aspartyl carboxylate that coordinates indirectly via a bridging water molecule (*48*, *50*). The liganding residues in the EF site differ at the $+z$ and $-x$ positions: Asp rather than Ser at the $+z$ position, Gly rather than Asp at the $-x$ position. In this paper, we discuss the alterations in Ca^{2+} binding that result from CD−EF interchange of the $+z$ and $-x$ ligands.

As is customary, single-site mutations are indicated with the residue number bracketed by the one-letter abbreviations for the original and substituted amino acids. Multiple mutations are indicated by simply listing the residue numbers separated by slashes, with the understanding that the mutations involve interchange of the CD and EF site residues. For example, 55/59 denotes the variant harboring the combined S55D and D59G mutations. The CD site in 55/59 is occasionally referred to as a "quasi-EF" site, since it has a ligand array identical to the authentic EF site. The EF site in the 94/98 variant is similarly referred to as a "quasi-CD" site.

In the following paragraphs, we first consider the impact of these mutations on protein stability. We then describe the Ca^{2+}-binding properties of each variant − beginning with the four single-site variants, followed by the two double-site variants (55/59 and 94/98), then 55/59/94, and finally the quadruple variant 55/59/94/98.

Differential scanning calorimetry (DSC) was used to assess the impact of these site-specific mutations on protein stability. The proteins were examined in their metal-free, or apo, forms to avoid complications in interpretation arising from altered Ca^{2+} affinity. Representative scans are presented in Figure 2 for wild-type OM, 55/59, 94/98, and 55/59/94/98. Melting temperatures (T_m) and enthalpies of denaturation (ΔH_d) for all of the proteins are listed in Table 1.

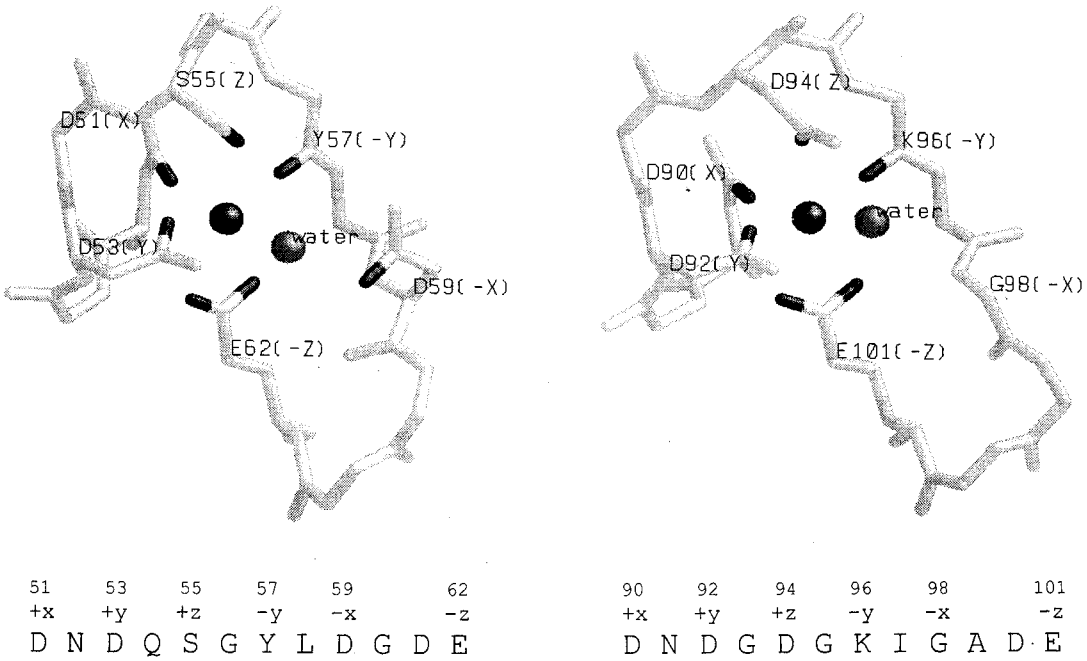

FIGURE 1: Comparison of the CD and EF site ligand arrays. These structural depictions of the CD (left) and EF (right) binding sites were generated with RasMol, v.2.6 (*47*), using the crystallographic data reported by Ahmed et al. (*48*). The amino acid sequence for each binding loop (*49*) is indicated below its respective structure.

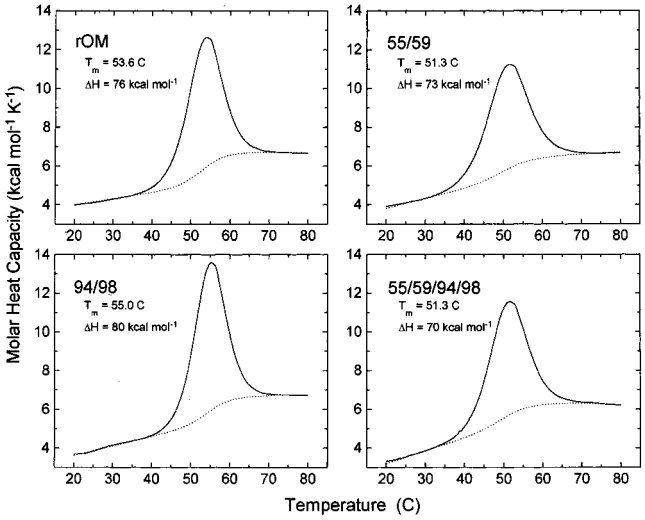

FIGURE 2: Differential scanning calorimetry on select OM variants. DSC analyses were performed as described under Materials and Methods.

Table 1: Summary of Thermal Stability Parameters

protein	T_m (°C)	ΔH_d (kcal mol^{-1})	ΔS (kcal mol^{-1} K^{-1})
wild-type OM	53.6	76 (4)	0.26
S55D	49.3	56 (3)	0.17
D59G	53.6	75 (4)	0.23
D94S	56.1	81 (4)	0.24
G98D	51.8	72 (3)	0.22
55/59	51.3	73 (3)	0.22
94/98	55.0	80 (4)	0.28
55/59/94	52.7	72 (3)	0.21
55/59/94/98	51.3	70 (3)	0.21

S55D and G98D both lower the T_m − by 4.3° and 1.8°, respectively. Conversely, D94S raises the T_m by 2.5 °C. Although D59G alone has no perceptible impact on stability, leaving the T_m unchanged at 53.6 °C, the mutation moderates the destabilizing influence of the S55D mutation in the 55/59 variant. The T_m measured for 55/59 (51.3 °C) is close to the average of the T_m's for the individual mutations (51.4 °C). The melting temperatures observed for 94/98 (55.0 °C) and 55/59/94 (52.7 °C) are similarly close to the averages for the individual mutations (54.0 and 53.0 °C, respectively). However, the T_m for 55/59/94/98 (51.3 °C) departs significantly from the average (53.2 °C).

With the exception of S55D, the enthalpies of denaturation are little changed in the variant proteins. Consistent with expectation, those proteins denaturing at a higher temperature than wild-type OM display a slightly elevated ΔH_d, while those denaturing at a lower temperature display a slightly reduced ΔH_d. The substantial reduction in ΔH_d observed for S55D suggests that this mutation may provoke relatively larger structural alterations.

Calcium-Binding Properties. Binding isotherms for wild-type OM and the single-site variants—S55D, D59G, D94S, and G98D—are displayed in Figure 3A. Corresponding data for the multiple-site variants—55/59, 94/98, 55/59/94, and 55/59/94/98—are displayed in Figure 3B. The binding parameters for each of the proteins—determined by flow-dialysis and titration calorimetry—are listed in Table 2. Dissociation constants were assigned by monitoring parallel Ca^{2+} titrations by NMR; the ^1H chemical shift values for Ca^{2+}-bound oncomodulin have been reported previously (*51*). To facilitate comparison, the coordinating residues in the CD and EF sites of each variant are also included in the table.

D59G. The Ca^{2+} dissociation constants that we measure for the EF and CD sites in wild-type OM are 45 and 800 nM, respectively (*31*), values similar to those reported by Cox et al. (*32*). Binding data for the D59G variant are displayed in Figure 3A (●), together with corresponding data for the wild-type protein (○). The dissociation constants obtained by least-squares analysis of three replicate titrations are 78 nM and 22 μM. Thus, the replacement of aspartate-59 by glycine reduces the Ca^{2+} affinity of the CD site by a

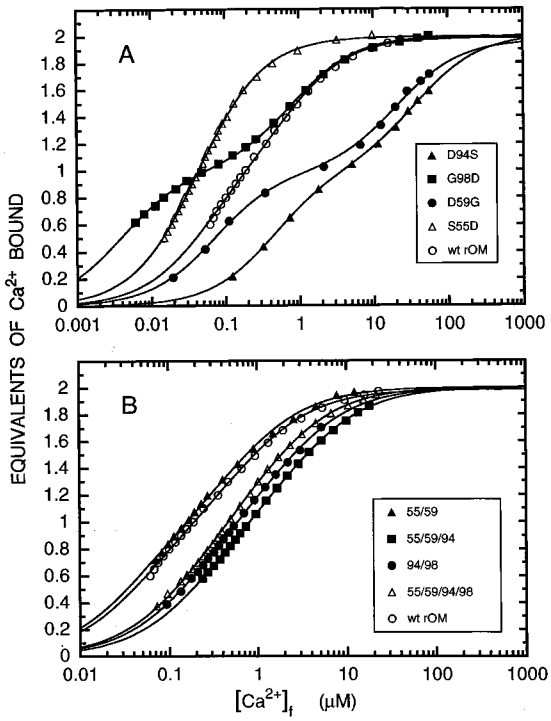

FIGURE 3: Binding of Ca^{2+} to OM variants. (A) Ca^{2+}-binding isotherms are presented for S55D (△), D59G (●), D94S (▲), and G98D (■), along with corresponding data for the wild-type protein (○). (B) Binding isotherms for 55/59 (▲), 94/98 (●), 55/59/94 (■), and 55/59/94/98 (△), and wild-type OM (○).

factor of 28 ($\Delta\Delta G = +2.0$ kcal/mol) and causes a slight reduction in the apparent affinity of the EF site as well ($\Delta\Delta G = +0.3$ kcal/mol).

When the titration of wild-type OM with Ca^{2+} is monitored calorimetrically (Figures 4A and 5A), we obtain apparent enthalpy changes for occupation of the EF and CD sites of -4.1 and -3.4 kcal/mol, respectively (*52*). Corresponding data for a representative titration of D59G are displayed in Figure 5B. It is evident that the mutation severely depresses the enthalpy change associated with binding at the CD site. The ΔH values that we extract for the binding events at the EF and CD sites are -4.7 and -1.3 kcal/mol, respectively. Thus, the overall $\Delta\Delta H$ resulting from the D59G mutation is $+1.5$ kcal/mol. This value is somewhat smaller than the overall $\Delta\Delta G$, suggesting that the reduction in affinity caused by the replacement of aspartate-59 with glycine has both enthalpic and entropic contributions.

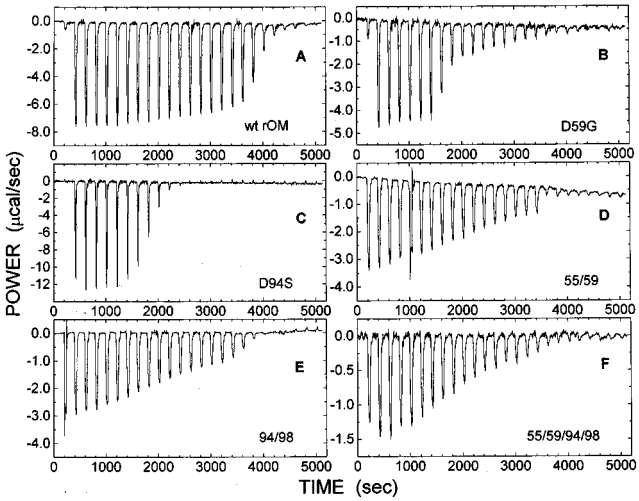

FIGURE 4: Raw titration data for OM and select OM variants. (A) Titration of 540 μM OM with 15 mM Ca^{2+}. (B) Titration of 210 μM D59G with 7.5 mM Ca^{2+}. (C) Titration of 420 μM D94S with 13 mM Ca^{2+}. (D) Titration of 285 μM 55/59 with 7.5 mM Ca^{2+}. (E) Titration of 412 μM 94/98 with 12 mM Ca^{2+}. (F) Titration of 250 μM 55/59/94/98 with 7.5 mM Ca^{2+}.

S55D. The binding isotherm resulting from replacement of serine-55, the $+z$ ligand in the CD loop, by aspartate is also displayed in Figure 3A (△). In contrast to the D59G mutation, S55D causes a significant increase in the Ca^{2+} affinity of the protein. The dissociation constants extracted from least-squares analyses of replicate experiments are 26 and 67 nM (*52*). ^{1}H NMR analysis indicates that these values reflect the binding events at the EF- and CD-binding sites, respectively. Thus, the S55D mutation elevates the Ca^{2+} affinity of the CD site by more than an order of magnitude and affords a slight increase in the affinity of the EF site. The "acid-pair" hypothesis, proposed by Reid and Hodges (*53*) on the basis of results obtained with peptide analogues (*54*−*56*), predicts that Ca^{2+} affinity should be maximized in an EF-hand having four carboxylates paired on the $+x$, $-x$ and $+z$, $-z$ axes. Introduction of a fifth carboxylate into the coordination sphere has been shown to reduce Ca^{2+} affinity in peptide model systems (e.g., *57*), presumably due to heightened interligand repulsion. Thus, the behavior observed for S55D was somewhat unexpected.

Titration calorimetry data for S55D, displayed in Figure 5C, indicate that the mutation increases the exothermicity associated with Ca^{2+} binding. The near-equality of the

Table 2: Summary of Calcium-Binding Data for OM and OM Variants[a]

	CD site					EF site				
protein	ligands[b]	K_{Ca} (μM)[c]	$\Delta G_{Ca}{}^{\circ\prime}$ [d]	ΔH	$-T\Delta S^{\circ\prime}$ [e]	ligands	K_{Ca} (μM)	$\Delta G_{Ca}{}^{\circ\prime}$	ΔH	$-T\Delta S^{\circ\prime}$
wild-type	D D S C═O D(w) E	0.80 (0.03)	−8.3 (0.1)	−3.4 (0.1)	−4.9	D D D C═O w E	0.045 (0.005)	−10.0 (0.1)	−4.1 (0.1)	−5.9
S55D	D D D C═O D(w) E	0.067 (0.012)	−9.7 (0.1)	−2.4 (0.2)	−7.3	D D D C═O w E	0.026 (0.005)	−10.3 (0.1)	−6.7 (0.1)	−3.6
D59G	D D D C═O w E	22 (2)	−6.3 (0.1)	−1.3 (0.1)	−5.0	D D D C═O w E	0.078 (0.02)	−9.7 (0.1)	−4.7 (0.1)	−5.0
D94S	D D S C═O D(w) E	0.50 (0.02)	−8.6 (0.1)	−4.3 (0.2)	−4.3	D D S C═O w E	42 (3)	−5.9 (0.1)	+0.2 (0.2)	−6.1
G98D	D D S C═O D(w) E	0.8 (0.04)	−8.3 (0.1)	−3.4 (0.1)	−4.9	D D D C═O D(w) E	0.004 (0.003)	−11.4 (0.1)	−4.0 (0.1)	−7.4
55/59	D D D C═O w E	0.72 (0.07)	−8.3 (0.1)	−0.3 (0.3)	−4.6	D D D C═O w E	0.045 (0.004)	−10.0 (0.1)	−5.1 (0.1)	−5.2
94/98	D D S C═O D(w) E	0.25 (0.02)	−9.0 (0.1)	−2.8 (0.1)	−6.2	D D S C═O D(w) E	3.0 (0.2)	−7.5 (0.1)	−0.8 (0.1)	−6.7
55/59/94	D D D C═O w E	0.23 (0.02)	−9.0 (0.1)	−1.9 (0.3)	−6.6	D D S C═O w E	12 (1)	−6.7 (0.1)	0 (0.2)	−4.9
55/59/94/98	D D D C═O w E	0.16 (0.02)	−9.2 (0.1)	−2.4 (0.1)	−6.7	D D S C═O D(w) E	1.3 (0.1)	−8.0 (0.1)	0 (0.2)	−7.4

[a] All energies are expressed in kcal/mol. [b] Ligands are listed from N- to C-terminus. One-letter amino acid abbreviations denote coordination by the corresponding side chain; C═O indicates the coordination by a main-chain carbonyl at the $-y$ position; w indicates coordination by a water molecule. D(w) indicates indirect coordination by an aspartyl carboxylate at the $-x$ position. [c] Apparent dissociation constant for Ca^{2+} binding. [d] $\Delta G_{Ca}{}^{\circ\prime} = -RT \ln(1/K_{Ca})$, where K_{Ca} is the corresponding Ca^{2+} dissociation constant. [e] $-T\Delta S^{\circ\prime} = \Delta G_{Ca}{}^{\circ\prime} - \Delta H$.

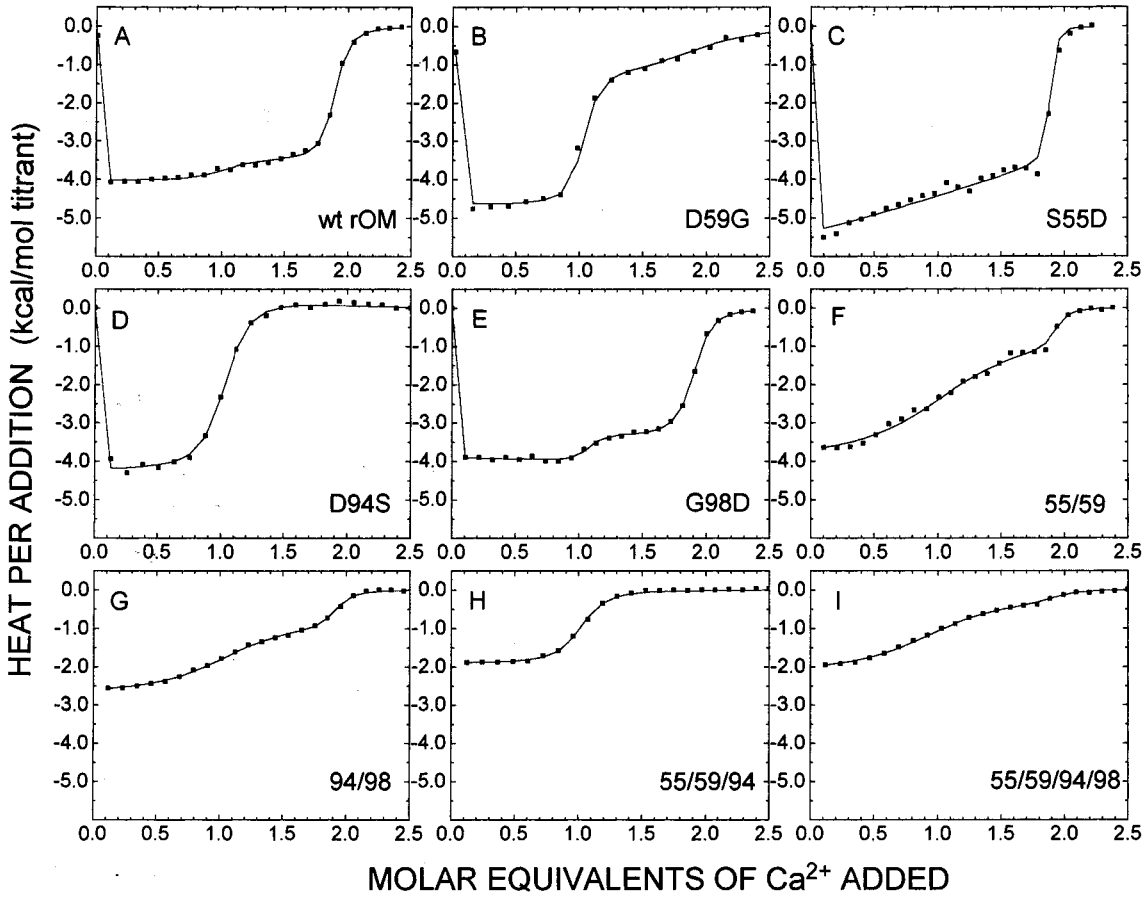

FIGURE 5: Heat of Ca^{2+} addition versus total Ca^{2+} added for wild-type OM and the OM variants. To facilitate comparison between experiments performed at different protein concentrations, data are reported per mole of titrant added. (A) Wild-type OM; (B) D59G; (C) S55D; (D) D94S; (E) G98D; (F) 55/59; (G) 94/98; (H) 55/59/94; (I) 55/59/94/98.

overall $\Delta\Delta G$ and $\Delta\Delta H$ values (Table 2 and *52*) suggests that the heightened affinity of S55D for Ca^{2+} has an enthalpic origin.

D94S. Representative Ca^{2+}-binding data for the D94S variant are plotted in Figure 3A (▲). Least-squares analysis of three replicate experiments afforded dissociation constants of 0.50 and 42 μM, respectively. Since a parallel titration monitored by ^{1}H NMR indicated that the order of occupancy is reversed in the D94S variant, the larger dissociation constant must correspond to the EF site. Thus, replacement of aspartate-94 (the +*z* ligand) by serine reduces the Ca^{2+} affinity of the EF site by nearly 3 orders of magnitude ($\Delta\Delta G$ = +4.1 kcal/mol). Notice that the D59G and the D94S mutations yield identical ligand arrays in the CD and EF sites, respectively, and that the Ca^{2+} affinities of these altered sites are comparably weak.

When the binding of Ca^{2+} to the D94S variant is monitored by titration calorimetry, we obtain the data presented in Figures 4C and 5D. Interestingly, the mutation virtually abolishes the enthalpy change associated with occupation of the weakened EF site. The apparent ΔH values for the CD and EF sites are −4.3 and +0.2 kcal/mol, respectively. In contrast to D59G, the unfavorable change in the enthalpy of Ca^{2+} binding ($\Delta\Delta H$ = +3.4 kcal/mol) is nearly equal to the overall loss of Ca^{2+} affinity ($\Delta\Delta G$ = +3.8 kcal/mol).

Although the reduction in Ca^{2+} affinity at the EF site resulting from the D94S mutation was anticipated, the increase in affinity at the CD site was unexpected. The dissociation constant for the CD site is reduced from 800 nM in the wild-type protein to 500 nM in D94S ($\Delta\Delta G$ = −0.3 kcal/mol). In the 94/98 variant (discussed below), the apparent CD site binding constant is further reduced to 250 nM. A qualitatively similar trend is noted below for the 55/59, 55/59/94, and 55/59/94/98 variants.

G98D. In contrast to the D94S mutation, replacement of glycine-98 in the EF site by aspartate substantially increases the Ca^{2+} affinity of the EF site. Binding data for G98D are displayed in Figure 3A (■). Least-squares analysis of replicate experiments yielded dissociation constants of 4 and 800 nM for the EF and CD sites, respectively. Like the S55D mutation in the CD site, the G98D substitution adds a fifth carboxylate to the coordination sphere of the EF site. Thus, the resultant gain in affinity, comparable to that seen in S55D, is likewise at odds with the acid-pair hypothesis.

Representative titration calorimetry data are presented in Figure 5E. The enthalpies for the Ca^{2+}-binding events at the CD and EF sites are estimated to be −3.4 and −4.0 kcal/mol, respectively, very similar to those determined for wild-type OM. Whereas the heightened affinity of the S55D variant has an enthalpic origin, the heightened affinity of the G98D variant apparently has an entropic origin (*52*).

55/59. Replacement of aspartate-59 by glycine in the S55D variant endows the CD site with a ligand array identical to that of the wild-type EF site. The Ca^{2+}-binding isotherm for 55/59 is displayed in Figure 3B (▲). The dissociation constants for the EF and CD sites extracted from three replicate experiments are 45 and 720 nM, respectively. Significantly, the Ca^{2+} affinity of the quasi-EF site created

in the CD-binding loop by the combined S55D and D59G mutations is markedly attenuated relative to the wild-type EF site. In fact, the affinity of the quasi-EF site is very similar to that determined for the wild-type CD site.

Raw calorimetry data for the titration of 55/59 with Ca^{2+} are displayed in Figure 4D. The integrated heat fluxes are plotted vs total Ca^{2+} added in Figure 5F. Least-squares analysis of these data afforded estimates of -5.1 and -0.3 kcal/mol for the enthalpies of binding to the EF and CD sites, respectively. Thus, relative to the wild-type protein, the enthalpy change associated with occupation of the EF site is perceptibly larger, while that associated with occupation of the engineered CD site, i.e., the quasi-EF site, is negligible.

Since the combined S55D and D59G mutations lower the T_m of the protein by 2.3 °C, the apo-form of the 55/59 variant might be somewhat less tightly folded than wild-type OM. Accordingly, occupation of the EF site in 55/59 would be accompanied by the formation of more numerous van der Waals interactions. By contrast, the markedly reduced enthalpy change associated with occupation of the quasi-EF site in 55/59 may reflect either a more limited conformational change than that occurring in the wild-type protein or an intrinsically weaker interaction with the bound ion.

94/98. Introduction of the D94S mutation into G98D, to afford the 94/98 variant, furnishes the EF site with a ligand array identical to that in the CD site. Ca^{2+}-binding data for 94/98 are displayed in Figure 3B (●). The dissociation constants that we obtained from replicate experiments are 0.25 and 3.0 μM. NMR data indicate that, as in the D94S variant, the order of occupancy of the binding sites is reversed relative to that observed in the wild-type protein, so that the 3.0 μM dissociation constant is associated with the altered EF site.

Although the ligands at the CD and EF sites of this variant are identical, the quasi-CD site resulting from the combined mutations at residues 94 and 98 has a somewhat lower apparent affinity for Ca^{2+} (K_d = 3.0 μM) than does the authentic CD site in wild-type oncomodulin (K_d = 0.80 μM). Significantly, the CD site ligand array does not acquire the high Ca^{2+} affinity characteristic of the wild-type EF site when placed at the C-terminal end of the molecule. As observed for the D94S variant, reversal of the order of occupancy yields a detectable increase in the measured affinity of the CD-binding loop for Ca^{2+} relative to the wild-type protein.

Raw titration calorimetry data for 94/98 are displayed in Figure 4E, and the integrated heat effects are plotted in Figure 5G. These two mutations in the EF site significantly depress the enthalpy changes associated with Ca^{2+} binding. The apparent ΔH_{Ca} values decrease from -4.1 and -3.4 kcal/mol, respectively, for the wild-type EF and CD sites to -0.8 and -2.8 kcal/mol for the corresponding sites in the 94/98 double variant.

55/59/94 harbors the serine→aspartate mutation at residue 55, the aspartate→glycine mutation at residue 59, and the serine→aspartate mutation at residue 94. Representative Ca^{2+}-binding data for the 55/59/94 variant are displayed in Figure 3B (■). The dissociation constants that we extract by least-squares analysis are 0.23 and 12 μM. ^{1}H NMR data indicate that the CD site is occupied first, so that the larger of the two constants must correspond to the EF site.

Recall that introduction of the D94S mutation into the wild-type protein increased the Ca^{2+} dissociation constant from 45 nM to 42 μM, a factor of nearly 10^3 ($\Delta\Delta G$ = +4.1 kcal/mol). When introduced into the 55/59 variant, D94S has a comparable impact, raising the apparent dissociation constant from 45 nM to 12 μM ($\Delta\Delta G$ = +3.3 kcal/mol). Notice further that introduction of the D94S mutation into 55/59 significantly decreases the Ca^{2+} dissociation constant for the remote CD site, from 0.72 μM to 0.23 μM. This behavior is qualitatively similar to that noted previously for the single-site D94S variant.

Titration calorimetry data for 55/59/94 are presented in Figure 5H. Recall that replacement of aspartate-94 by serine in the wild-type protein profoundly alters the enthalpy change associated with Ca^{2+} binding in the EF site ($\Delta\Delta H$ = +4.1 kcal/mol). A similar effect is observed upon introducing the D94S mutation into the 55/59 variant. The ΔH value shifts from -5.1 kcal/mol for the EF site of 55/59 to 0 for the corresponding site in 55/59/94. The enthalpy change associated with binding at the CD site becomes somewhat more exothermic, shifting from -0.3 kcal/mol to -1.9 kcal/mol.

55/59/94/98. The combined mutations at residues 55, 59, 94, and 98 exchange the ligand arrays in the CD and EF sites. Ca^{2+}-binding data for the 55/59/94/98 variant are displayed in Figure 3B (△). The best least-squares fit to a two-site model yields dissociation constants of 160 nM and 1.3 μM. ^{1}H NMR data indicate that the smaller dissociation constant corresponds to the CD site. Recall that introduction of G98D into the wild-type EF site increases the apparent affinity of that site by a factor of 11 and that introduction of G98D into D94S yields a 12-fold increase in affinity. The mutation similarly affords a 9-fold increase in the affinity of the EF site when incorporated into the 55/59/94 background.

Raw Ca^{2+} titration calorimetry data for 55/59/94/98 are presented in Figure 4F, and the corresponding integrated heat effects are plotted against the total Ca^{2+} concentration in Figure 5, panel I. The best least-squares estimates for ΔH are -2.4 kcal/mol and 0 for the CD and EF sites, respectively.

DISCUSSION

In general, parvalbumin CD and EF sites behave equivalently during titrations with Ca^{2+}, exhibiting dissociation constants between 1 and 10 nM at physiological pH and ionic strength. However, the CD and EF sites in oncomodulin are a notable exception, differing in Ca^{2+} affinity by a factor of 20. We have undertaken these studies to assess the relevance of higher order structural considerations, namely, placement of the binding loop within the protein sequence, to this issue. Specifically, we wished to determine (1) whether the oncomodulin EF site coordination sphere retains its high-affinity signature when imported into the CD binding loop and (2) whether the oncomodulin CD site coordination sphere experiences a marked increase in affinity when transplanted to the C-terminal end of the molecule.

To address these questions, we produced a site-specific variant of OM having two EF-like ligand arrays (55/59), as well as one having two CD-like ligand arrays (94/98). In addition, we exchanged the CD and EF ligand arrays to produce 55/59/94/98. The relative performance of the wild-type and engineered binding sites in these two proteins offers some insight into the significance of flexibility on the performance of the two ligand arrays. In addition to these

multiple-site variants, we have also characterized each of the single-site variants. Before examining the impact of these mutations on Ca^{2+} affinity, we briefly discuss the effect of the mutations on the conformational stability of the apoform of the protein.

Thermal Stability. The four individual mutations examined in this study—S55D, D59G, D94S, and G98D—are fairly conservative, and all occur in solvent-exposed regions of the protein. With the exception of S55D, they confer modest alterations in stability, less than 2.5 °C.

The consequences of these mutations are largely consistent with straightforward electrostatic arguments. OM has a predicted charge of −16 at pH 7.4. Since the S55D and G98D mutations introduce an additional charge, they are expected to aggravate electrostatic repulsion in the protein, thereby decreasing the stability of the native state. Accordingly, both lower the melting point of the protein. The somewhat greater destabilization caused by S55D (a 4.3 °C reduction in T_m and a 20 kcal/mol reduction in the enthalpy of denaturation) suggests that this substitution may cause a local unfolding of the protein, with concomitant exposure of apolar surface area.

Conversely, since D59G and D94S both eliminate a formal charge, they are predicted to stabilize the native state. Consistent with this expectation, D94S raises the melting temperature by 2.5 °C. Interestingly, however, the D59G mutation does not similarly increase the T_m. Some additional factor must counterbalance the more favorable electrostatic free energy.

The wild-type CD site and the engineered EF site in 94/98 have the identical constellation of ligands. Replacement of the $+z$ serine with aspartate in the CD site (to afford S55D) lowers the T_m by 4.3 °C. The same replacement in the EF site of 94/98 (to produce G98D) lowers the T_m by 3.2 °C, suggesting that the stability of the molecule is more sensitive to alterations at the $+z$ position in the CD site. By contrast, replacement of the $-x$ aspartate by glycine in the CD site (to afford D59G) has no impact on the melting temperature, while the same mutation in the EF site of 94/98 (to yield D94S) stabilizes the protein by 1.1 °C.

In general, the thermal behavior of the multiple-site variants is a composite of the individual mutations. Thus, the destabilizing influence of S55D is tempered somewhat by the D59G mutation in the 55/59 variant. Similarly, the stabilizing influence of the D94S mutation is moderated by the G98D mutation in 94/98. In both cases, the observed T_m is very close to the average of the two individual mutations. Although this same trend is continued in 55/59/94, the melting temperature of the quadruple variant 55/59/94/98 is roughly 2 °C lower than the average of the four individual mutations.

Ca^{2+}-Binding Properties of the Single-Site Variants. The S55D and G98D variants have been discussed in a previous study (*52*). Their Ca^{2+}-binding properties are recapitulated here to facilitate the discussion of the multiple-site variants. As described in the earlier work, both mutations introduce an additional carboxylate into their respective ligand arrays, and both increase the Ca^{2+} affinity of their host sites by an order of magnitude. Interestingly, in the case of S55D, the increased affinity has an enthalpic origin, whereas the increased Ca^{2+} affinity of G98D reflects an increase in the entropy of binding.

Aspartate-94, the $+z$ ligand in the EF-binding loop, is directly coordinated to the bound Ca^{2+} ion. Replacement by serine increases the apparent dissociation constant for the EF site from 45 nM to 42 μM, a reduction in the Ca^{2+} affinity by nearly 3 orders of magnitude. Titration calorimetry data indicate that the decrease in the free energy of binding is almost entirely enthalpic, i.e., $\Delta\Delta H = +3.4$ kcal/mol, quite similar to the $\Delta\Delta G$ value of +3.8 kcal/mol.

There are three potential causes for the decreased exothermicity of Ca^{2+} binding in this variant. Crystallographic data suggest that the nonliganding carboxylate oxygen in D94 interacts with the ϵ-ammonium group of K96 (*48*, *50*). The substitution of serine at position 94 would eliminate this enthalpically favorable interaction in the Ca^{2+}-bound form. Alternatively, the less favorable enthalpy of binding in D94S might reflect an attenuated interaction between the EF site ligands and the bound Ca^{2+} per se. Although the driving force for Ca^{2+} chelation is assumed to be largely entropic, the enthalpy change for replacement of the hydration shell by the chelatory ligand array is generally nonzero. A third explanation for the reduction in magnitude of ΔH is that the conformational rearrangement that accompanies the binding of Ca^{2+} to D94S is reduced.

Although aspartate-59 is the $-x$ liganding residue in the CD site, the γ-carboxylate does not coordinate directly to the bound Ca^{2+}. Rather, it is indirectly liganded via an intervening water molecule. In the D59G variant, a water molecule also occupies the $-x$ position of the CD site inner coordination sphere. Thus, the replacement of aspartate-59 by glycine does not change the proximal ligand. Nevertheless, the Ca^{2+} affinity of the CD site is reduced by a factor of 25 ($\Delta\Delta G = +2.3$ kcal/mol). Intuitively, one might anticipate that this decrease would have a significant entropic contribution, since a glycyl residue would experience a greater loss of configurational entropy than aspartate in the Ca^{2+}-bound state. Consistent with expectation, the D59G mutation is accompanied by a $-T\Delta\Delta S$ term for Ca^{2+} binding of +0.8 kcal/mol.

The D59G mutation also causes a significant decrease in the exothermicity of Ca^{2+} binding ($\Delta\Delta H = +1.5$ kcal/mol). According to the crystal structure determined for OM (*48*, *50*), the aspartate-59 carboxylate is hydrogen-bonded neither to the peptide backbone nor to a neighboring side chain. Thus, substitution by glycine is not expected to reduce the number of stabilizing hydrogen bonds in the Ca^{2+}-bound form. It is more likely that the decreased enthalpic contribution mirrors the weaker interaction between the bound Ca^{2+} and the unperturbed water molecule in D59G, relative to the interaction of the ion with the bridging water molecule in the wild-type CD site.

Drake and Falke (*58*) have performed detailed equilibrium and kinetic studies of lanthanide binding to the model EF-hand site in the *E. coli* galactose-binding protein. Replacement of aspartate by glycine in that system reduces the affinity of the protein for Tb^{3+} by a factor of 11. Their data indicate that replacement of a negatively charged side chain at the $-x$ position with a neutral side chain reduces the ground-state stability of the bound state and lowers the transition energy barrier to dissociation. Because the kinetics of Ca^{2+} binding and release can be tuned over a wide range by simply varying the identity of the $-x$ ligand, they refer to the $-x$ residue as the "gateway residue."

Ca^{2+}-Binding Properties: Multiple-Site Variants. The combination of the S55D and D59G mutations within the CD-binding loop imbue the CD site with a ligand array identical to that found in the EF loop. The relative Ca^{2+} affinities of these two sites—the "quasi-EF site" and the wild-type EF site—illustrate the performance of this ligand constellation in the relatively flexible C-terminal region and in the more rigid central region. If the affinity of the EF site were dictated exclusively by local factors, i.e., ligand identity, the two sites in 55/59 should behave equivalently during Ca^{2+} titrations. Interestingly, however, placement of the EF site ligand array into the CD-binding loop is accompanied by a marked reduction in affinity: The apparent Ca^{2+} dissociation constants of the wild-type EF site and the quasi-EF site in the 55/59 variant are 45 and 720 nM, respectively. Thus, the engineered site exhibits substantially lower affinity for Ca^{2+}, in fact, approaching that of the wild-type CD site, suggesting that placement of the EF site ligand array in the relatively rigid central region compromises its performance. In fairness, however, it should be recognized that the latter value is substantially inflated by the negatively cooperative interaction between the two sites (vide infra). The dissociation constant of 160 nM determined for the quasi-EF site in the 55/59/94/98 variant may offer a better estimate of the intrinsic Ca^{2+} affinity of the ligand array in this setting. Nevertheless, even this amended value suggests that the potential binding affinity of the EF-site ligand array cannot be realized in the structural context of the oncomodulin CD loop.

As mentioned in the introduction, Cox and his colleagues have suggested that the relatively low affinity of the OM CD site is dictated largely, if not exclusively, by the amino acid sequence of residues 41−70 (*36*, *37*). The failure of the EF site ligand array to retain its high-affinity signature when imported into the CD domain is certainly consistent with their proposal. In this context, it would be interesting to examine the 55/59 double mutation in other parvalbumin backgrounds, notably in rat α-PV, which possesses a high-affinity CD site, and in avian parvalbumin CPV3, in which the CD site exhibits intermediate Ca^{2+} affinity (*59*).

Just as the combined S55D and D59G mutations permit comparison of the EF site ligand array in the central and C-terminal regions of the molecule, the combined D94S and G98D mutations likewise permit comparison of the CD ligand array in the two distinct environments. Assuming that the attenuated Ca^{2+} affinity displayed by the OM CD site is indeed dictated primarily by the amino acid sequence spanning residues 41−70, then the CD site ligand array should acquire a high-affinity phenotype when imported into the EF domain. Somewhat unexpectedly, it retains a low-affinity signature. The apparent K_d (3.0 μM) for the quasi-CD site created in the EF-binding loop of 94/98 is roughly 4 times larger than that determined for the wild-type CD site (0.8 μM). If allowance is made for negative cooperativity, the apparent difference in Ca^{2+} affinity is smaller still. Thus, unlike the OM EF site array, the behavior of the OM CD site ligand array appears to be largely insensitive to placement, less sensitive than the EF ligand array to its environment.

However, the question immediately arises as to whether the combined D94S and G98D mutations would behave similarly in other PV backgrounds. Moreover, the presence of aspartate at the $-x$ position in the CD site distinguishes OM from all other known PV isoforms. Since glutamate is the consensus residue at this position, it would also be of interest to learn whether the quasi-CD site resulting from the combined D94S and G98E mutations mimics the quasi-CD site in D94S/G98D or whether it in fact displays higher affinity for Ca^{2+}.

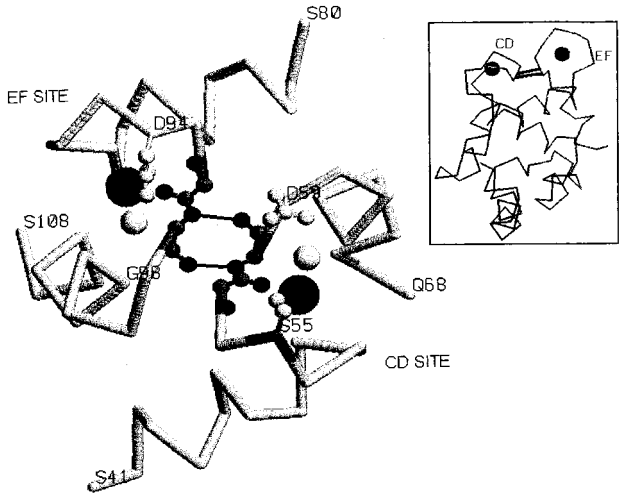

FIGURE 6: Spatial orientation of the parvalbumin CD- and EF-binding sites. The CD and EF sites, related by an approximate 2-fold symmetry axis, are physically linked by a short segment of antiparallel β-sheet. Hydrogen bonds between L58 and I97 are indicated in black. The bound Ca^{2+} ions; the relative positions of residues 55, 59, 94, and 98; and the aquo ligands that occupy the $-x$ coordination positions have also been indicated. The relationship of the two binding sites to the remainder of the molecule is shown in the inset. This figure was prepared with RasMol (*47*) using the published crystallographic coordinates for oncomodulin (*48*).

The overall ΔH values for Ca^{2+} binding observed for several of the variants deserve comment. The total ΔH for the 55/59 variant is just −5.4 kcal/mol. This value is 2.1 kcal/mol less exothermic than that observed for wild-type OM, even though the overall ΔG for Ca^{2+} binding is unchanged. Similarly, whereas the overall ΔH for binding of Ca^{2+} to the 94/98 variant is 3.9 kcal/mol less favorable than in the wild-type protein, the binding free energy is changed by just +1.8 kcal/mol. Finally, the overall ΔH for Ca^{2+} binding to 55/59/94/98 is a mere −2.4 kcal/mol—5.1 kcal/mol less favorable than in wild-type OM—although the change in the free energy of binding is just +1.1 kcal/mol. Since the overall Ca^{2+} affinity is largely preserved in these three proteins, the reductions in magnitude of ΔH suggest that the conformational changes that accompany Ca^{2+} binding to the variants are more limited than in the wild-type protein.

Cooperativity. It is generally assumed that the parvalbumin CD and EF sites are independent and noninteracting. However, as DiCera (*60*) points out, this conclusion—largely based on the observation of linear Scatchard plots and Hill coefficients near unity—is unwarranted. The dissection of site−site interactions in systems comprising intrinsically nonequivalent sites is far from trivial.

The spatial relationship between the parvalbumin CD- and EF-binding sites is depicted in Figure 6. As in other paired EF-hand motifs, there is clearly the potential for site−site interactions. The two sites are physically adjacent—with the bound Ca^{2+} ions just 12 Å apart—and connected by a short segment of antiparallel β-sheet formed by residues within

the metal ion-binding loops. This structural element provides a straightforward mechanism for transmitting structural information between the two sites. Hydrogen bonds are present between the amide hydrogen of L58 and the carbonyl oxygen of I97 and between the carbonyl oxygen of L58 and the amide hydrogen of I97. Ca^{2+}-induced conformational alterations within the EF site, for example, could be readily propagated to the CD loop by these interactions. In this context, whiting parvalbumin is reported to bind Ca^{2+} in a positively cooperative manner (*61*).

Sykes, MacManus, and co-workers have previously suggested that metal ion binding by oncomodulin is cooperative in nature (*62*). Their conclusion was based primarily on ^{1}H NMR and stopped-flow analysis of $Ca^{2+}-Lu^{3+}$ exchange data for wild-type OM and the D59E variant. By monitoring NMR resonances specific for the CD and EF sites, they concluded, for example, that the D59E mutation increased the Lu^{3+} affinity of *both* binding sites in OM by a factor of 5. The binding studies presented here offer further evidence for conformational interactions between the oncomodulin CD and EF sites.

In wild-type OM, the EF site is occupied first during Ca^{2+} titrations, due to its intrinsically higher affinity for Ca^{2+}. Consequently, the Ca^{2+} ion subsequently coordinated at the CD site binds primarily to a conformation dictated by the binding event at the EF site. However, in several of the above-mentioned variants, notably D94S and 94/98, the Ca^{2+} affinity of the EF site has been weakened to the point that the order of occupancy is reversed. Significantly, the Ca^{2+} affinity of the CD site is increased in these variants. For example, the Ca^{2+} dissociation constant for the CD site is reduced from 800 nM in the wild-type protein to 500 nM in D94S and further reduced to 230 nM in 94/98. These data suggest that the binding of Ca^{2+} to OM is negatively cooperative—i.e., occupation of the EF site antagonizes the subsequent binding event at the CD site. The $\Delta\Delta G$ value of -0.7 kcal/mol calculated for the CD site of the 94/98 variant (Table 2) suggests that the magnitude of this unfavorable interaction is on the order of 1 kcal/mol.

In the 55/59 variant, the CD-binding loop has acquired a ligand array identical to that in the wild-type EF site. Nevertheless, this altered CD site retains sensitivity to mutations in the EF site, comparable to that observed for the wild-type CD site. As in wild-type OM, the EF site of 55/59 is occupied preferentially in titrations with Ca^{2+}, and the D94S and 94/98 mutations similarly reverse the order of occupancy. Significantly, the Ca^{2+} dissociation constant for the CD site in the 55/59 variant decreases from 570 nM in the 55/59 variant to approximately 230 nM in 55/59/94 and to 160 nM in 55/59/94/98. This trend further implies that the binding events at the wild-type CD and EF sites are mutually antagonistic. The $\Delta\Delta G$ value of -0.9 kcal/mol calculated for the CD site in the 55/59/94/98 variant, relative to the CD site in 55/59, likewise suggests that the magnitude of the negatively cooperative interaction is roughly 1 kcal/mol.

Summary. Whereas the oncomodulin EF site displays a high-affinity (or Ca^{2+}/Mg^{2+}) phenotype, the CD site is a low-affinity (Ca^{2+}-specific) site. The CD and EF ligand arrays differ at the $+z$ and $-x$ positions. We have examined the consequences of exchanging these residues, both singly and in pairs, with the intent of exploring the relative importance of ligand identity on Ca^{2+} affinity. The D59G and D94S mutations, both of which eliminate a carboxylate ligand from the coordination, substantially reduce Ca^{2+} affinity. By contrast, the S55D and G98D mutations, both of which introduce a fifth carboxylate into the coordination sphere, heighten Ca^{2+} affinity. The latter observations are in conflict with data previously gathered on model peptide systems.

The combined S55D and D59G mutations create an EF site ligand array in the context of the CD-binding loop. Significantly, the EF array exhibits a substantial reduction in Ca^{2+} affinity when imported into the CD site, suggesting that the CD site environment is not optimal for this constellation of liganding residues. Conversely, the combined D94S and G98D mutations create a CD site ligand array in the context of the EF site. Interestingly, the CD ligand array does not acquire a high-affinity phenotype upon transfer to the EF site environment, suggesting that the Ca^{2+} affinity of this constellation of ligands is relatively insensitive to placement within the protein molecule. Oncomodulin is distinguished from other parvalbumins by its unusually low isoelectric point (p$I = 3.1$) and sequence eccentricities (e.g., Y57-L58-D59 instead of F57-I58-E59). It will be interesting to learn whether CD−EF ligand exchange has similar consequences in other parvalbumin isoforms from both the α and β sublineages.

Finally, we observe that the Ca^{2+} affinity of the CD site is perceptibly increased by mutations that reduce the Ca^{2+} affinity of the EF site. This finding suggests that the affinity of the oncomodulin CD for the Ca^{2+} site is attenuated in part by a negatively cooperative interaction with the EF site.

REFERENCES

1. McPhalen, C. A., Strynadka, N. C. J., and James, M. N. G. (1991) *Adv. Protein Chem. 42*, 77−144.
2. Kawasaki, H., and Kretsinger, R. H. (1995) *Protein Profile 2*, 297−490.
3. Falke, J. J., Drake, S. K., Hazard, A. L., and Peersen, O. B. (1994) *Q. Rev. Biophys. 27*, 219−290.
4. Linse, S., and Forsén, S. (1995) *Adv. Second Messenger Phosphoprotein Res. 30*, 89−151.
5. Wnuk, W., Cox, J. A., and Stein, E. A. (1982) *Calcium Cell Funct. 2*, 243−278.
6. Gerday, C. (1988) in *Calcium and Calcium-binding Proteins. Molecular and Functional Aspects* (Gerday, C., Bollis, L., and Gilles, R., Eds.) pp 23−39, Springer-Verlag, Berlin.
7. Pauls, T. L., Cox, J. A., and Berchtold, M. W. (1996) *Biochim. Biophys. Acta 1306*, 39−54.
8. Berchtold, M. W. (1996) in *Guidebook to the Calcium-Binding Proteins* (Celio, M., Pauls, T., and Schwaller, B., Eds.) pp 123−128, Oxford University Press, Oxford.
9. Haiech, J., Derancourt, J., Pechère, J.-F., and Demaille, J. G. (1979) *Biochemistry 18*, 2752−2758.
10. Moeschler, H. J., Schaer, J.-J., and Cox, J. A. (1980) *Eur. J. Biochem. 111*, 73−78.
11. Serda, R., and Henzl, M. T. (1991) *J. Biol. Chem. 266*, 7291−7299.
12. Eberhard, M., and Erne, P. (1994) *Eur. J. Biochem. 222*, 21−26.
13. Williams, T. C., Corson, D. C., and Sykes, B. D. (1984) *J. Am. Chem. Soc. 106*, 5698−5702.
14. Goodman, M., and Pechère, J.-F. (1977) *J. Mol. Evol. 9*, 131−158.
15. Moncrief, N. D., Kretsinger, R., and Goodman, M. (1990) *J. Mol. Evol. 30*, 522−562.
16. Heizmann, C. W (1988) in *Calcium and Calcium Binding Proteins. Molecular and Functional Aspects* (Gerday, C., Bolis, L., and Gilles, R., Eds.) pp 93−101, Springer-Verlag, Berlin.

17. Heizmann, C. W., Berchtold, M. W., and Rowlerson, A. M. (1982) *Proc. Natl. Acad. Sci. U.S.A. 79*, 7243−7247.
18. Müntener, M., Kaser, L., Weber, J., and Berchtold, M. W. (1995) *Proc. Natl. Acad. Sci. U.S.A. 92*, 6504−6508.
19. Plogman, D., and Celio, M. R. (1993) *Brain Res. 600*, 273−279.
20. Celio, M. R. (1986) *Science 231*, 991−997.
21. Celio, M. R. (1990) *Neuroscience 35*, 375−475.
22. Sloviter, R. S. (1989) *J. Comput. Neurol. 280*, 183−196.
23. Thalmann, I., Shibasaki, O., Comegys, T. H., Henzl, M. R., Senarita, M., and Thalmann, R. (1995) *Biochem. Biophys. Res. Commun. 215*, 142−147.
24. Henzl, M. T., Shibasaki, O., Comegys, T. H., Thalmann, I., and Thalmann, R. (1997) *Hear. Res. 106*, 105−111.
25. Sakaguchi, N., Henzl, M. T., Thalmann, I., Thalmann, R., and Schulte, B. A. (1997) *J. Histochem. Cytochem.* (in press).
26. MacManus, J. P., Brewer, L. M., and Whitfield, J. F. (1985) *Cancer Lett. 27*, 145−151.
27. MacManus, J. P., Brewer, L. M., and Banville, D. (1990) *Adv. Exp. Med. Biol. 269*, 107−110.
28. MacManus, J. P., and Whitfield, J. F. (1983) *Calcium Cell Funct. 4*, 411−440.
29. MacManus, J. P., Brewer, L. M., and Gillen, M. F. (1987) in *Role of Calcium in Biological Systems* (Anghileri, L. J., Ed.) pp 1−19, CRC Press, Boca Raton, FL.
30. Blum, J. K., and Berchtold, M. W. (1994) *J. Cell. Physiol. 160*, 455−462.
31. Hapak, R. C., Lammers, P. L., Palmisano, W. A., Birnbaum, E. R., and Henzl, M. T. (1989) *J. Biol. Chem. 264*, 18751−18760.
32. Cox, J. A., Milos, M., and MacManus, J. P. (1990) *J. Biol. Chem. 265*, 6633−6637.
33. Williams, T. C., Corson, D. C., Sykes, B. D., and MacManus, J. P. (1987) *J. Biol. Chem.* 262, 6248−6256.
34. Palmisano, W. A., Treviño, C. L., and Henzl, M. T. (1990) *J. Biol. Chem. 265*, 14450−14456.
35. Treviño, C. L., Boschi, J. M., and Henzl, M. T. (1991) *J. Biol. Chem. 266*, 11301−11308.
36. Pauls, T. L., Durussel, I., Clark, I. D., Szabo, A. G., Berchtold, M. W., and Cox, J. A. (1996) *Eur. J. Biochem. 242*, 249−255.
37. Durussel, I., Pauls, T. L., Cox, J. A., and Berchtold, M. W. (1996) *Eur. J. Biochem. 242*, 256−263.
38. Kauffman, J. F., Hapak, R. C., and Henzl, M. T. (1995) *Biochemistry 34*, 991−1000.
39. Deng, W. P., and Nickoloff, J. A. (1992) *Anal. Biochem. 200*, 81−88.
40. Haner, M., Henzl, M. T., Raissouni, B., and Birnbaum, E. R. (1984) *Anal. Biochem. 138*, 229−234.
41. Colowick, S. P., and Womack, F. C. (1968) *J. Biol. Chem. 244*, 774−776.
42. Cox, J. A. (1996) in *Guidebook to the Calcium-Binding Proteins* (Celio, M., Pauls, T., and Schwaller, B., Eds.) pp 1−12, Oxford University Press, Oxford.
43. Freire, E., Mayorga, O. L., and Straume, M. (1990) *Anal. Chem. 62*, 950−959.
44. Christensen, J. J., Hansen, L. D., and Izatt, R. M. (1976) *Handbook of Proton Ionization Heats and Related Thermodynamic Quantities*, John Wiley and Sons, New York.
45. Briggner, L.-E., and Wadsö, I. (1991) *Biochem. Biophys. Methods 22*, 101−118.
46. Griesinger, C., Otting, G., Wüthrich, K., and Ernst, R. R. (1988) *J. Am. Chem. Soc. 110*, 7870−7872.
47. Sayle, R., and Milner-White, E. J. (1995) *Trends Biochem. Sci. 20*, 374.
48. Ahmed, F. R., Rose, D. R., Evans, S. V., Pippy, M. E., and To, R. (1993) *J. Mol. Biol. 230*, 1216−1224.
49. Gillen, M. F., Banville, D., Rutledge, R. G., Narang, S., Seligy, V. L., Whitfield, J. F., and MacManus, J. P. (1987) *J. Biol. Chem. 262*, 5308−5312.
50. Ahmed, F. R., Przybylska, M., Rose, D. R., Birnbaum, G. I., Pippy, M. E., and MacManus, J. P. (1990) *J. Mol. Biol. 216*, 127−140.
51. Henzl, M. T., Likos, J. J., and Hutton, W. C. (1996a) *Protein Pept. Lett. 3*, 59−66.
52. Henzl, M. T., Hapak, R. C., and Goodpasture, E. A. (1996b) *Biochemistry 35*, 5856−5869.
53. Reid, R. E., and Hodges, R. S. (1980) *J. Theor. Biol. 84*, 401−444.
54. Reid, R. E. (1987) *Biochemistry 26*, 6071−6073.
55. Reid, R. E. (1990) *J. Biol. Chem. 265*, 5971−5976.
56. Procyshyn, R. M., and Reid, R. E. (1994) *Arch. Biochem. Biophys. 311*, 425−429.
57. Marsden, B. J., Hodges, R. S., and Sykes, B. D. (1988) *Biochemistry 27*, 4198−4206.
58. Drake, S. K., and Falke, J. J. (1996) *Biochemistry 35*, 1753−1760.
59. Hapak, R. C., Zhao, H., Boschi, J. M., and Henzl, M. T. (1994) *J. Biol. Chem. 269*, 5288−5296.
60. Di Cera, E. (1995) *Thermodynamic Theory of Site-Specific Binding Processes in Biological Macromolecules*, Cambridge University Press, Cambridge.
61. White, H. D. (1988) *Biochemistry 27*, 3357−3365.
62. Golden, L. F., Corson, D. C., Sykes, B. D., Banville, D., and MacManus, J. P. (1989) *J. Biol. Chem. 264*, 20314−20319.

BI973151W